CALCULATION OF ELECTRON CONTAMINATION IN A ^{60}Co THERAPY BEAM

D.W.O. ROGERS, G.M. EWART, A.F. BIELAJEW
Physics Division,
National Research Council of Canada,
Ottawa, Ontario

G. VAN DYK
Atomic Energy of Canada Limited,
Kanata, Ontario

Canada

Abstract

CALCULATION OF ELECTRON CONTAMINATION IN A ^{60}Co THERAPY BEAM.

The EGS Monte Carlo radiation transport system has been used to model the therapy beam from an AECL ^{60}Co unit. Photon contamination is shown to be mostly due to the source capsule and to have little effect on the depth-dose curve. The calculations for broad beams show that there are many sources of electron contamination (collimators, air, source capsule) which vary in importance as a function of SSD. The effects of filters and magnets on electron contamination have been studied. The calculations are shown to be in good agreement with experimental results except very close to the surface (<0.5 mm) where the calculations underestimate the measurements.

1. Introduction

Electron contamination of broad ^{60}Co therapy beams can increase the maximum dose by up to 15% and can shift the depth of dose maximum from 5 mm to 1 mm. There have been a variety of both theoretical and experimental investigations of this effect (e.g. [1] to [4] and references therein) and it is now well established that electrons are the major contaminant. However, there has been no comprehensive study for ^{60}Co beams which could distinguish the various sources of electron contamination. To investigate the possibilities for reducing this contamination and as a first step in the development of a general Monte Carlo model of an accelerator head, we have modelled a ^{60}Co unit. There has been considerable previous work on modelling the photon contamination in a ^{60}Co therapy unit (see e.g. [5]) but prior to this work ([6]) there has been little study of the effects of the photons on the buildup region. There have been some comparable studies related to electron contamination of accelerator photon beams [7].

From Proceedings of the Symposium on Dosimetry in Radiotherapy, Vol 1, (IAEA, Vienna, 1988).

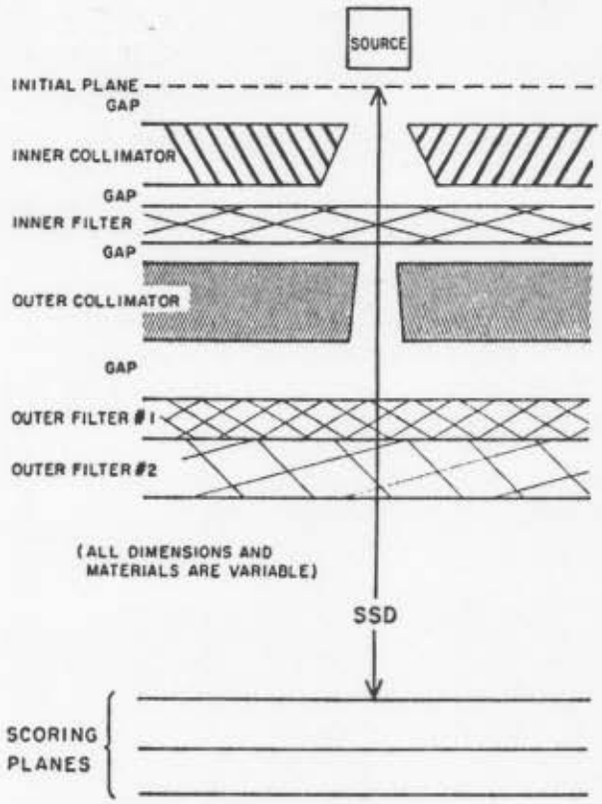

FIG. 1. The geometry modelled. There is cylindrical symmetry. The source can be a point source, parallel beams or pre-computed output from the ^{60}Co capsule in Fig. 2.

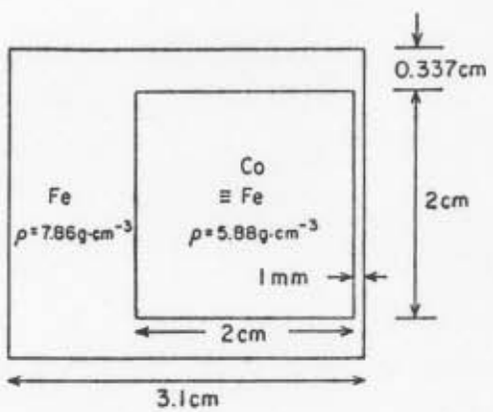

FIG. 2. Model used for the encapsulated ^{60}Co source.

2. Calculations

The model uses the EGS Monte Carlo system to simulate the transport of electrons and photons [8]. EGS takes into account photo-electric, Compton and pair production interactions of photons and accounts for the slowing of electrons, the creation of secondary photons and electrons and the multiple scattering of electrons. It was found essential to use a reduced electron step-size to obtain accurate results (see [9]).

Figure 1 presents a schematic of the geometry which was modelled. It was essential to model fully the ^{60}Co source capsule which is shown in figure 2. This was done separately and the phase space parameters of 2 million electrons and photons entering the beam collimation system from the front face of the capsule were stored in a highly compressed format and used repeatedly as input to the rest of the simulation.

The computer code is general but for the purposes of this study a "BASE" case has been defined which represents a broad beam from an AECL therapy unit (Theratron 780, which is rectangular rather than cylindrical as modelled). The inner collimator is solid lead, and fixed to allow an unobstructed beam of up to 39.5 cm diameter at an SSD of 80 cm (equal in area to a 35 x 35 cm^2 beam). It is 1.50 cm from the capsule, 6.2 cm thick, with inner and outer radii of 1.4 and 2.68 cm. The outer collimators pivot on a hinge at the inner corner of the inner collimator and are adjusted to define the field size via a line through the center of the capsule face and the outer edge of the outer collimator. The hinge was not modelled and the outer collimator was taken to be solid although in reality it is made of leaves. It was 19.3 cm thick, made of lead, 0.4 cm past the inner collimator and had inner and outer radii of 2.77 and 6.76 cm in the BASE case. The BASE case included no filters or magnets although they could be included either between the collimators or anywhere between the unit and the patient plane by terminating all electron histories entering the magnet region.

To make the calculation tractable required the use of a wide variety of variance reduction techniques, including: i) calculating the effects of the source capsule and repeatedly using the stored results; ii) forcing all photons to interact in the air or the filters before leaving the head and using appropriate weights to account for the extra interactions; iii) terminating the history of any electron unable to reach the patient; iv) forcing all primary photons leaving the head to interact in the air outside the head; v) reusing all particles leaving the head for calculations at each SSD being considered; and vi) calculating depth-dose curves by scoring the planar fluence at the patient surface and folding these with pre-computed depth-dose curves for normally incident mono-energetic particles [10,11]. For low energy photons it was essential to use pre-computed depth-dose curves [11] which included details of the buildup curves. When pre-computed curves were used which did not take into account the buildup in the first 2 mm [10], the low energy photons appeared to contribute significantly to the surface dose.

The variance reduction techniques increase the computing efficiency by up to a factor of 100. To obtain electron depth-dose curves with a few percent statistical

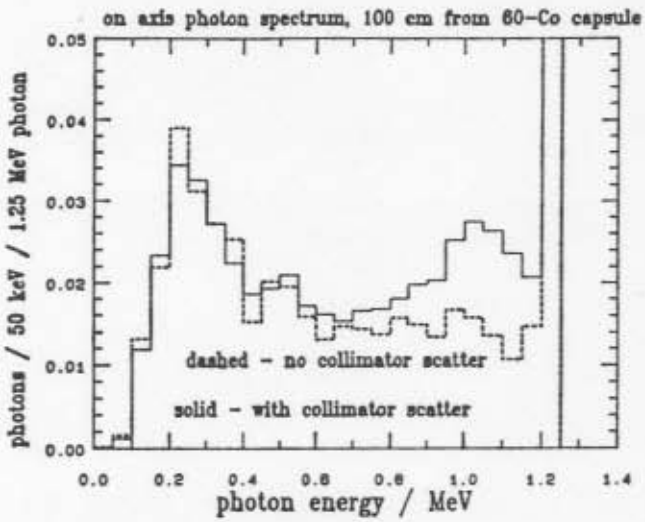

FIG. 3. On-axis photon spectra, 100 cm from the source capsule, with and without the effects of collimator and air scatter.

uncertainty required 5 to 16 hours of VAX/780 CPU time. With the exception of using the pre-computed depth-dose curves, these techniques do not affect the accuracy of the simulation. Using pre-computed depth-dose curves introduces two approximations since they are assumed to be broad and incident normally. These assumptions affect the surface dose somewhat, but have little effect at depths of 1 mm or greater (see [12] and below). One final approximation was that electrons were tracked down to 100 keV and then considered to deposit all their energy on the spot. The range of these electrons is about 14 mg·cm^{-2} in water and 13 cm in air.

3. Results

3.1. Scattered photons

The major source of scattered photons is the source capsule itself, as is shown in Figure 3. The scattered photons contribute 29% of the on-axis fluence or 18% of the maximum dose. The electrons from the capsule have an average energy of 580 keV and represent only 0.5% of the particles leaving the front face. These can still have a large effect on the dose in the buildup region as we shall see below. If we also consider the photons scattered from the collimators, the scatter component goes up to about 32% of the fluence as seen in Figure 3 and Table I.

Table I

On-axis photon spectrum from a ^{60}Co unit in the BASE case configuration, including capsule, collimator and air scatter. The values are normalized absolutely per initial 1.25 MeV photon in the source capsule (multiply by 2 to get Bq^{-1}). One standard deviation uncertainties are given in brackets.

Top of bin (MeV)	Photons/sr/MeV/ 1.25 MeV photon	Top of bin (MeV)	Photons/sr/MeV/ 1.25 MeV photon
0.05	≈ 0	0.65	0.0176 (2%)
0.10	0.0013 (10%)	0.70	0.0168 (3%)
0.15	0.0130 (3%)	0.75	0.0181 (3%)
0.20	0.0256 (3%)	0.80	0.0183 (4%)
0.25	0.0376 (3%)	0.85	0.0197 (2%)
0.30	0.0355 (2%)	0.90	0.0216 (3%)
0.35	0.0297 (3%)	0.95	0.0222 (4%)
0.40	0.0245 (4%)	1.00	0.0276 (2%)
0.45	0.0203 (4%)	1.05	0.0300 (2%)
0.50	0.0212 (2%)	1.10	0.0288 (3%)
0.55	0.0229 (3%)	1.15	0.0259 (2%)
0.60	0.0188 (3%)	1.20	0.0223 (2%)
		1.25	1.094 (<0.5%)

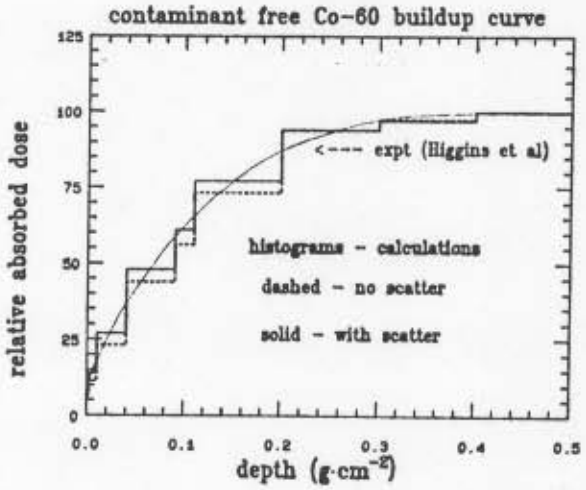

FIG. 4. Comparison of the measured [13] and calculated buildup curves for photon beams with no electron contamination.

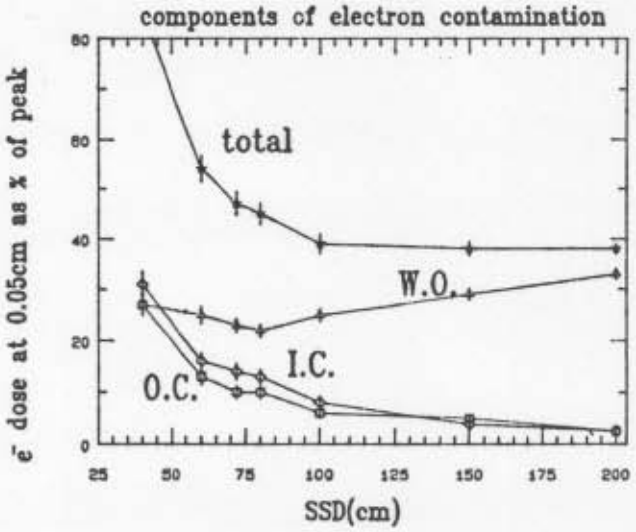

FIG. 5. Components of electron contamination as a function of SSD in the BASE case (39.5 cm diameter, unfiltered beam).

At dose maximum, about 1% and 4% of the dose comes from photons scattered from the inner and outer collimators, respectively. This result means that our model is incapable of explaining the roughly 10% increase in dose rate observed in clinical photon beams as the beam size increases. At most a 5% increase can be caused by increased collimator scatter. The remainder of the increase must be related to other factors, perhaps a partial blocking of the source with smaller field sizes. Figure 4 presents a comparison of our calculated results with the measurements of Higgins et al. [13] for the buildup region of a beam with no electron contamination. Including scattered photons in the calculations makes a small improvement in the comparison. Scattered photons are found to have only a small effect on the overall depth-dose curve.

3.2. Electron contamination

3.2.1. BASE case

On account of multiple scattering and creation of knock-on electrons etc, it is quite difficult to define uniquely "where an electron came from". In figure 5, we have separated the electron contamination into several components. The **'W.O.'** (within outer) component consists of all electrons from electrons or photons which leave the source capsule in a direction within the outer collimator (i.e. in the beam). This component includes the electrons from the capsule and

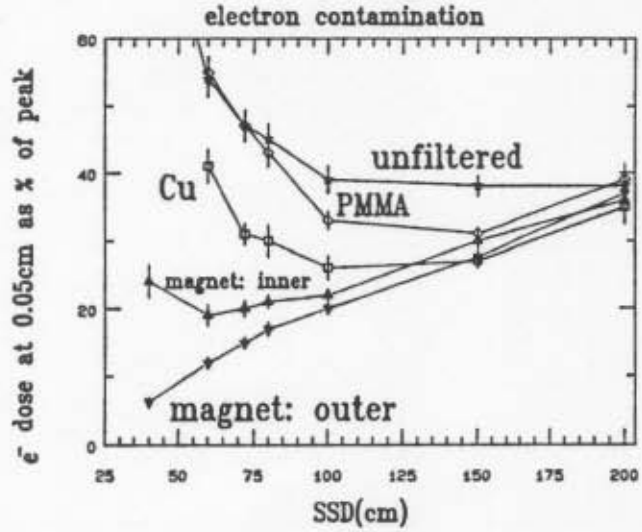

FIG. 6. Electron contamination versus SSD for a variety of configurations of filters and magnets.

those generated in the air by photons. The 'I.C.' and 'O.C.' components are from those particles which leave the capsule headed for the inner collimator and outer collimator, respectively. Figure 5 presents the components of the electron contamination in the BASE case at 0.05 cm depth as a fraction of the peak dose in a water phantom as a function of SSD. The depth-dose curve resulting from electrons does not vary much at depths from 0.01 cm to 0.15 cm and is roughly the same shape for each component so that figure 5 gives an accurate indication of the overall electron contamination. This figure shows, for example, that at an SSD of 80 cm the contaminant electrons are 45% of the peak photon dose; 22% come from capsule and air generated electrons; 10% and 13% come from particles initially going towards the outer and inner collimators respectively. To get an idea of the electrons generated by the air only, one can look at the "magnet outer" curves in figure 6. We have investigated the effects of changing the collimator material and the collimator geometry somewhat. Electron contamination is virtually independent of material and somewhat dependent on details of the geometry. See reference [6] for a detailed discussion.

3.2.2. Filtered beams

We have investigated the effects of various filters on electron contamination. Figure 6 presents the results as a function of SSD for 0.7 g·cm^{-2} filters of PMMA or Cu placed at an SSD of 57 cm. These filters are thick enough to stop all contaminant electrons in the beam while only attenuating the photon beam by about 3%. However, they are themselves a source of electrons. Copper makes

a better filter because about 40% fewer electrons leave the Cu per transmitted photon. This is because the electrons are much more scattered in the copper and hence have a shorter effective range. This larger scatter also means that those electrons which do escape are less likely to reach the patient. We have investigated the effects of filter position and thickness(see [6]). There is no dramatic dependence on filter thickness. At an SSD of 80 cm the optimum distance for a Cu filter is 27 cm from the source but at SSD=100 cm there is little variation with filter position.

3.2.3. Magnets

Figure 6 also shows the effects of perfect electron sweeping magnets placed either between the collimators ("inner") or just outside the head ("outer"). The "outer" case shows the contamination caused by electrons generated in the air outside the therapy head. The "inner" case is almost as good as the "outer" case at typical treatment distances of 80 to 100 cm, but is much easier to implement because of the smaller dimensions of the beam at this point. With the advent of practical high temperature superconducting magnets this option may become more attractive.

3.2.4. Field size

All of the calculations reported above were for large diameter beams. For technical reasons we could only do preliminary runs for small field sizes. However, in agreement with experiment, we find that electron contamination in a 5 x 5 cm^2 field is 5 to 15 times less than in the broad beam case.

4. Comparison with experiment

We have compared our results with many of the measurements reported by Attix et al. [3] and in general find very good agreement except at the very surface (<0.5 mm). Figure 7 shows a comparison of the total dose at two depths vs SSD in a broad, unfiltered beam. The agreement at 0.1 $g{\cdot}cm^{-2}$ is good at all SSDs, but the calculations underestimate the dose at the surface. To investigate the limitations of using the pre-computed, normally incident depth-dose curves, we have done the much more time consuming "full" calculation at an SSD of 200 cm where only air generated electrons are important. Here the electrons were followed down to 10 keV and full account was taken of their non-normal incidence on the phantom. The points marked "full" in figure 7 demonstrate that the approximate methods work well at the greater depths, but they are somewhat inaccurate at the very surface. However, even the full calculation does not agree well with the experimental results for the very surface. In practical terms this is of no consequence because the dose is relatively small there, and these depths are still within the dead layer of the patient's skin. Nonetheless these discrepancies are unexplained and represent one of the worst cases of disagreement we have found

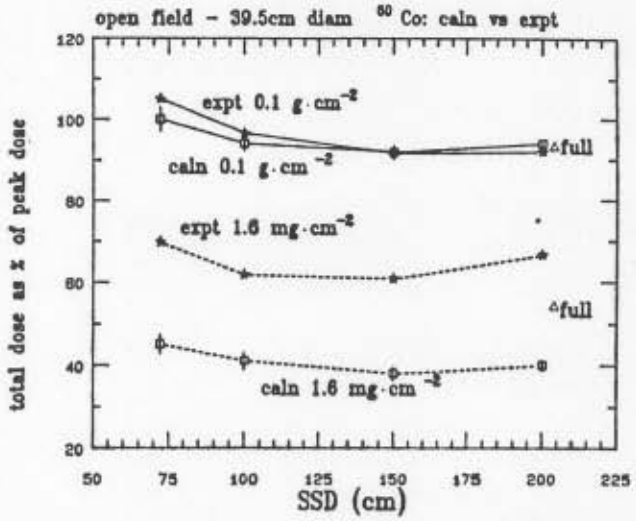

FIG. 7. Comparison for the BASE case between the calculations and measurements of Attix et al. [3]. The triangles marked 'full' are calculations for which the pre-computed depth-dose curves were not used and electrons were tracked to 10 keV.

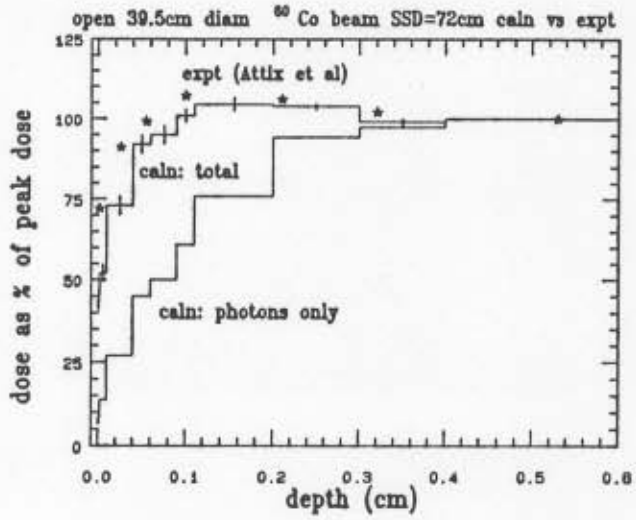

FIG. 8. Comparison of the calculated and measured [3] depth-dose curves at an SSD of 72 cm for the BASE case. The calculated dose for photons only is also shown.

between Monte Carlo calculations and experimental results. The disagreement may be the result of problems with the experimental results at the very surface; they may be explained by a slight offset in the depth scale; or they may represent theoretical problems in calculating the dose at an interface.

Figure 8 shows a comparison of the complete depth-dose curves as calculated and measured. From figure 7, it can be seen that this is the depth of worst agreement. Yet it is clear that the calculations go a long way towards explaining the electron contamination. Reference [6] presents many comparisons for filtered beams which also show good agreement.

5. Conclusions

The Monte Carlo code described here has been used to demonstrate that electron contamination explains the changes in the buildup region of a broad ^{60}Co therapy beam. Photon contamination is primarily from the source capsule, contributes significantly to the dose, but has little effect on the shape of the depth-dose curve. The electron contamination comes from a wide variety of places but the capsule itself is the major source at close SSDs and air generated electrons dominate at larger distances. Agreement with experiment is excellent except near the surface.

References

(1) Nilsson, B., Brahme, A., Phys.Med.Biol. 24(1979)901.
(2) Higgins, P.D., Sibata, C.H., Attix, F.H., Paliwal, B.R., Med.Phys. 10(1983)622.
(3) Attix, F.H., Lopez,F., Owalabi,S., Paliwal,B.R., Med.Phys. 10 (1983) 301.
(4) Galbraith,D.M., Rawlinson, J.A., Med.Phys.12 (1985)273-280.
(5) ICRU Report 18. *"Specification of High Activity Gamma-ray Sources"* ICRU, Washington D.C. (1970)
(6) Rogers, D.W.O., Bielajew, A.F., Ewart, G.M., van Dyk, G., *"Calculation of Contamination of the ^{60}Co Beam from an AECL Therapy Source"*, NRC Report PXNR-2710, Jan. 1985 (available from the authors); and Med. Phys.11 (1984) 401 and 12 (1985) 515, abstracts.
(7) Petti, P.L., Goodman, M.S., Sisterson, J.M., Biggs, P.J., Gabriel, T.A., Mohan, R., Med. Phys.10 (1983) 856-861.
(8) Nelson, W.R., Hirayama, H., Rogers, D.W.O., *"The EGS4 Code System"*, Stanford, Calif. (1985) SLAC Report-265.
(9) Rogers, D.W.O., Nucl. Instr. Meth. A227 (1984)535-548.
(10)Rogers, D.W.O., Health Phys. 46 (1984) 891-914.
(11)Rogers, D.W.O., Bielajew, A.F., Med. Phys. 12 (1985) 738-744.
(12)Rogers, D.W.O., Bielajew, A.F., *"The Use of EGS for Monte Carlo Calculations in Medical Physics"*, NRC Report PXNR-2692, (June 1984).
(13)Higgins, P.D., Sibata,C.H., Paliwal, B.R., Phys.Med.Biol. 30 (1985) 153-162.